

Sodium compatibility of ODS steel at elevated temperature

Eiichi Yoshida ^{*}, Shoichi Kato

O-arai Engineering Center, Japan Nuclear Cycle Development Institute (JNC), 4002, Narita, O-arai, Ibaraki 311-1393, Japan

Abstract

As oxide dispersion strengthened (ODS) ferritic steels have excellent resistance to swelling as well as superior mechanical strength, they are expected to be used as a long life cladding in the future advanced fast reactor. In this study, sodium environmental effects on the ODS steel developed by JNC were clarified through corrosion and mechanical tests in sodium at elevated temperature. For stagnant sodium conditions, sodium environmental effects were negligibly small. For flowing sodium condition at temperature over 948 K, however, nickel concentration increased at the surface of ODS steel, where phase transformation from α to γ was observed. In the γ -phase ODS steel, an oxide particle distribution is still maintained. From a simulation of the formation of γ -phase at the outer surface of an ODS steel cladding, it is concluded that its tensile strength could not be affected by sodium exposure, even in flowing sodium condition.

© 2004 Elsevier B.V. All rights reserved.

1. Introduction

Evaluation of sodium environmental effects on mechanical strength properties is essential to assure structural integrity throughout the designed life-time in sodium cooled fast reactors. Fuel claddings are particularly affected by sodium, since the cladding is extremely thin and operating temperatures are very high [1]. Therefore, it is important to understand the compatibility of materials with sodium at elevated temperatures.

In this study, sodium environmental effects on oxide dispersion strengthened (ODS) steels [2–4], a potential cladding material for the advanced future fast reactors, were investigated by corrosion and mechanical strength testing at elevated temperatures in a sodium environment.

2. Experimental procedure

2.1. Test materials

In this study, six types of the ODS steels were examined: five types of the ODS steels developed by

JNC (JNC-ODS steel) and one commercially available ODS steel (MA957) as a reference. Table 1 shows the chemical compositions of the tested materials. The JNC-ODS steels are in the shape of claddings and MA957 is a rolled plate type. These ODS steels are produced by the mechanically alloying method after finely dispersing Y_2O_3 oxide particles in steels, which have excellent swelling resistance and high temperature strength [3].

2.2. Corrosion test

Corrosion tests were performed on specimens set into a cyclic flowing sodium passage with heated and cooled parts (hereinafter ‘sodium flowing test’), and on specimens exposed in the sodium test vessel at constant temperature (hereinafter ‘sodium immersion test’). Both test sections of sodium loop were made of Type 316 austenitic stainless steel. Fig. 1(a) shows a diagram of the corrosion test section in the sodium flowing tests. The tests were performed for about 4600 h at a maximum flow rate of 5.1 m/s and at temperature from 873 to 973 K. The sodium immersion tests were performed with a flow rate of less than 0.001 m/s at 923 and 973 K for a maximum of 10 000 h. The oxygen concentration in the sodium was kept below 2 ppm using a cold trap system. After the corrosion tests, the change in the

^{*} Corresponding author. Tel.: +81-29 267 4141; fax: +81-29 267 0579.

E-mail address: e-yoshi@oec.jnc.go.jp (E. Yoshida).

Table 1
Chemical compositions of ODS steel (mass %)

	C	Si	Mn	Ni	Cr	Mo	Ti	W	Y ₂ O ₃ ^a
MA957	0.02	0.04	0.038	0.13	13.90	0.31	1.00	–	0.27
63DSA	0.02	0.03	0.020	0.12	12.80	–	0.74	2.75	0.46
F95	0.06	0.03	0.048	0.03	11.72	–	0.31	1.92	0.24
F11	0.02	0.05	0.046	0.03	11.95	–	0.30	2.01	0.24
M93	0.12	0.02	0.036	0.02	8.99	–	0.20	1.94	0.35
M11	0.13	0.05	0.044	0.02	9.01	–	0.21	1.95	0.36

^a Estimated from yttrium content assuming it is contained in the form of Y₂O₃.

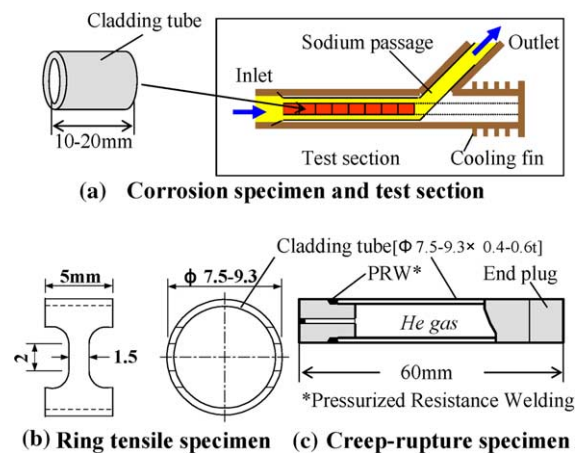


Fig. 1. Specimens used for corrosion, ring tensile and creep-rupture tests.

microstructure and composition of tests specimen was examined by the optical microscopy and electronic microscopy (TEM).

2.3. Tensile and creep-rupture tests

The tensile tests were processed using a ring shape specimen as shown in Fig. 1(b). Before the tensile tests, the specimens were pre-exposed in the sodium immersion tests condition. The tensile test was performed at the same temperature as the sodium immersion test under atmospheric surroundings. The strain rate is 0.1 mm/min for all tests.

Internal pressure creep tests were performed in sodium at 923 and 973 K for maximum 20 000 h by filling inside of the specimen with helium gas at the target pressure. The flow rate of sodium is less than 0.001 m/s. The oxygen concentration in sodium was kept below 2 ppm. Fig. 1(c) shows a specimen for the creep-rupture test under internal pressure. Fracture of the specimen was identified by detecting the helium gas released from inside of the specimen.

3. Experimental results

3.1. Corrosion behavior

Fig. 2(a) shows the weight change of specimens after corrosion tests. In the sodium flowing test condition, all specimens showed a trend towards increased weight, being particularly noticeable at higher temperatures. For the sodium immersion test conditions, although an increase in weight was observed, the extent of increase was smaller than that in sodium flowing test conditions.

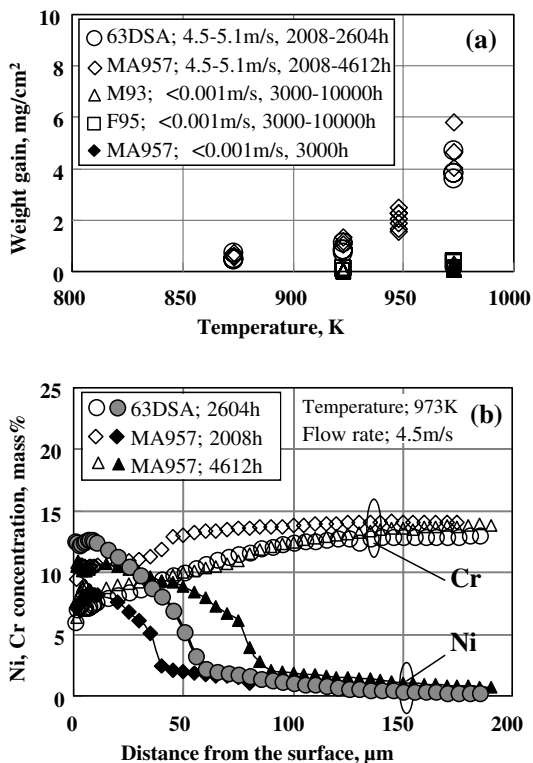
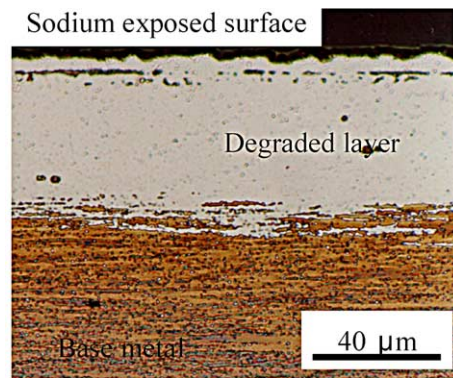


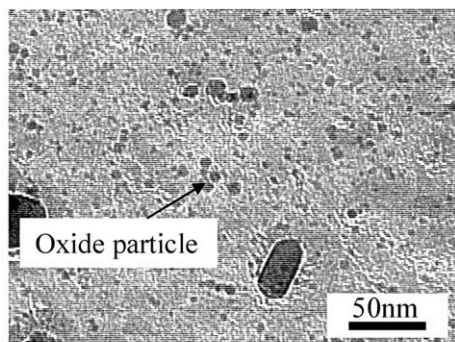
Fig. 2. Results of sodium corrosion test. (a) Weight change after corrosion test and (b) typical result of Ni diffusion for the ODS steel in sodium.

Fig. 2(b) shows the concentration distribution of nickel and chromium in a cross-section of 63DSA and MA957 claddings after exposed in the flowing sodium at 973 K. Increase in nickel concentration and decrease in chromium concentration were observed in response to the microstructure change (see Fig. 3(a)). For titanium and tungsten, no change in concentration was observed. Similarly, no change was confirmed for yttrium, oxygen and Y_2O_3 oxide particles, and the dissolution phenomena in sodium did not occur. These findings agreed with the following TEM observations.

Fig. 3 shows representative cross-section and TEM microstructures of 63 DSA cladding after the corrosion tests. For the sodium flowing test conditions, clear microstructure change (Fig. 3(a), hereinafter ‘surface degraded layer’) in several tens of microns was observed in the specimens whose surface were contacted with sodium. It was seen that the depth of surface degraded layer corresponds to the concentration change of nickel and it had dependency on temperature and sodium-exposure time. From X-ray diffraction results, a phase transformation from α to γ was seen in the surface degraded layer. In addition, fine Y_2O_3 oxide particles were



(a) Cross-sectional microstructure



(b) TEM micrograph of degraded layer region

Fig. 3. Microstructures of ODS steel after exposure flowing sodium (4.5 m/s) at 973 K.

observed within the surface degraded layer (Fig. 3(b)) as well as in the internal microstructure of steel, indicating that they remained stable in sodium. For the specimens of the sodium immersion tests where weight increase was not significant, clear microstructural change was not observed.

3.2. Mechanical properties

The results of tensile tests at high temperatures after the sodium immersion tests are shown in Fig. 4(a). Ultimate tensile strength (UTS) of martensitic M93 showed a downward trend in strength with increasing sodium-exposure duration. On the other hand, UTS of ferritic F95 remained almost constant up to sodium exposures of 10 000 h. For fracture elongation, no significant difference was confirmed. For conventional ferritic steel without Y_2O_3 , a clear strength reduction occurred above 873 K due to decarburization phenomena in sodium [5,6]. While decarburization was observed, the ODS steel did not show such a clear strength reduction in contrast to conventional steel even when exposed at a high temperature for a long time. This suggested that the fine Y_2O_3 oxide particles remained stable in steel and thus the strength mechanism of the steel was maintained. Fig. 4(b) shows the results of the creep-rupture tests with internally pressurized specimens under sodium immersion condition. Creep-rupture

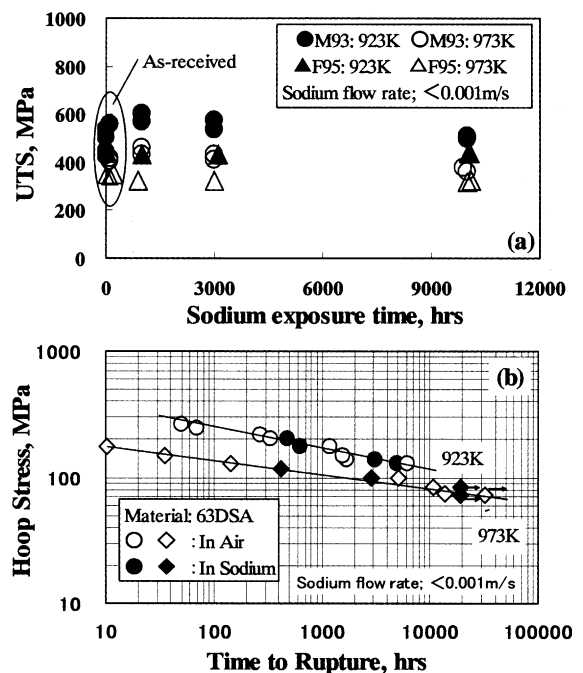


Fig. 4. Mechanical strength properties of ODS steel in sodium. (a) Ultimate tensile strength and (b) creep-rupture strength under internal pressure.

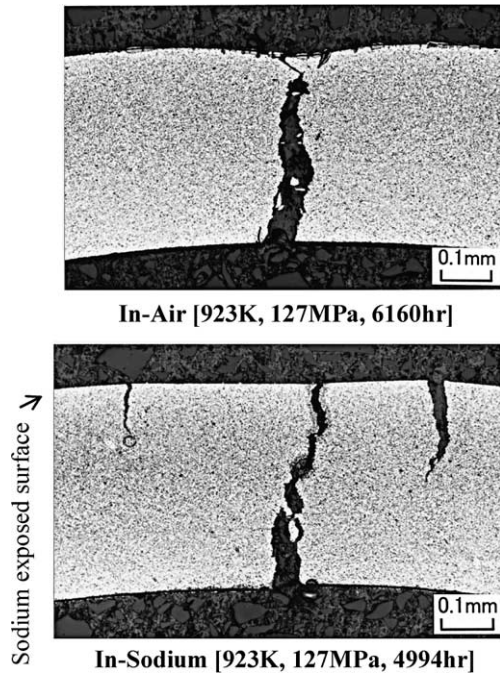


Fig. 5. Typical cross-sectional microstructures of ODS steel (63DSA) after creep-rupture tests.

strength in sodium was equal to the strength in air, and no sodium environmental effect is observed. The same is true for the creep-rupture ductility.

Fig. 5 shows a typical cross-sectional microstructure of a creep-ruptured specimen in sodium as compared with those in air. In both cases, creep cracks occurred from the inside of claddings and progresses until fracture. This behavior is supported by a general stress distribution evaluation. Given that the cracks occur from the inner wall, it is unlikely that the exposed sodium affects the crack initiation.

These mechanical tests suggest that sodium environmental effects can be ignored under stagnant conditions. However, as the fuel claddings are used in a high flow rate condition, it is necessary to consider the effects of microstructure change associated with nickel diffusion as observed in the sodium flowing tests.

4. Discussion

In corrosion conditions in sodium at high temperatures, austenitic stainless steels show the typical mass transfer behavior caused by a temperature difference. The major alloy elements such as nickel, chromium, manganese and silicon are dissolved into sodium in the higher temperature section that induces weight loss, and these elements precipitate and deposit at the lower temperature section causing weight gain [7]. In case of

the ODS steel, the weight gain is noticeable at higher temperature section, where the surface degraded layer is formed and nickel concentration increases at the sodium exposed surface. This phenomenon is observed for both the ferritic and martensitic ODS steels under flowing sodium environment. These nickel came from the Type 316 walls of the sodium testing loop. The nickel dissolved from Type 316 circulates through the testing loop, and diffuse into the ODS steel at the high temperature section. The amount of nickel diffusion is dominated by the difference of nickel activity in the exposed surface of the ODS steel and that in the sodium.

The coefficient of nickel diffusion in the ODS steel can be estimated based on the results of nickel concentration measurement in the corrosion tests. The results are shown in Fig. 6, where results of nickel diffusion treatment specimen are incorporated. These specimens were prepared by coating the surface of claddings with pure nickel, and then heated up in inert gas atmosphere to diffuse the nickel across the wall direction from the outer surface to wall thickness (t) of claddings between about $1/10t$ and $1/3t$. The nickel diffusion coefficient D of the ODS steel can be derived from the nickel concentration distribution through the wall direction.

$$D = D_0 \times \exp(-Q/RT),$$

where the frequency coefficient is $D_0 = 9.371 \times 10^{-9}$ [m^2/s], the activation energy is $Q = 145.784$ [K J/mol], the gas constant is $R = 8.3145$ [J/K/mol] and temperature is T [K]. This D value of the ODS steel is larger than that of a typical α -Fe steel at temperature below 973 K [8].

The relationship of mechanical properties with microstructure change caused by nickel diffusion was experimentally studied using artificial nickel diffused test

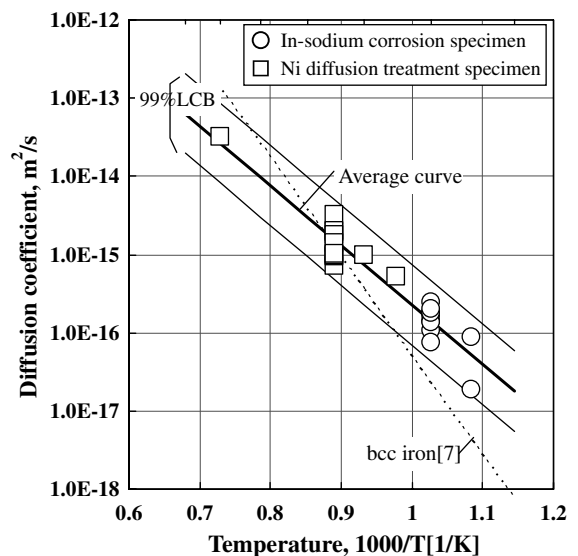


Fig. 6. Ni diffusion of ODS steel in flowing sodium.

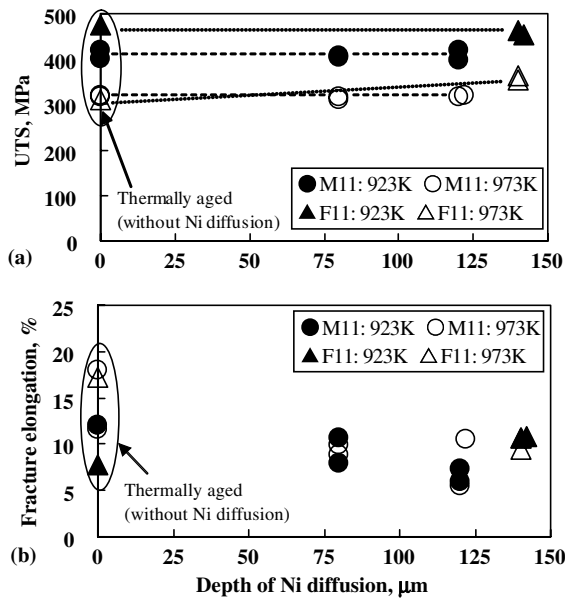


Fig. 7. Influence of Ni diffusion on tensile properties.

specimens. The relationship between tensile properties and depth of nickel diffusion for M11 and F11 are shown in Fig. 7. The UTS values of the nickel diffused test specimens are almost equal to those of only thermally aged specimen. The surface degraded layer produced by nickel diffusion, which is shown in Fig. 3, is probably maintained in strength by the fine Y_2O_3 oxide particles in the ODS steel. In other words, the effect of nickel diffusion against tensile properties is negligible. From these tests simulating the nickel diffusion into the ODS steel, it is concluded that tensile properties of the ODS steels could not be affected by sodium exposure even in the high velocity flowing condition.

5. Conclusions

The compatibility of the ODS steel in sodium was experimentally studied. The results showed excellent sodium-resistance up to a high temperature of about 973 K in stagnant sodium conditions, and the effects of sodium on tensile and creep properties were negligible. In flowing sodium conditions, the weight increase due to nickel diffusion into the ODS steel was observed at temperatures over 923 K, and a microstructure change associated with the phase transformation from α to γ was detected. However, the fine Y_2O_3 oxide particles, which constitute the strength mechanism of the ODS steel remained and were assumed to be stable in sodium. The tensile properties of nickel diffused test specimens at high temperatures simulating microstructure change were equal to that of the thermal aging process material.

References

- [1] Y. Kani, Y. Sagayama, in: Proceedings of Symposium: Energy and the Environment – The Role of Nuclear Power, Michigan, 2002, p. 139.
- [2] S. Ukai, M. Fujiwara, *J. Nucl. Mater.* 307–311 (2002) 749.
- [3] S. Ukai, S. Mizuta, M. Fujiwara, T. Okuda, T. Kobayashi, *J. Nucl. Sci. Technol.* 39 (7) (2002) 778.
- [4] S. Ukai, T. Okuda, M. Fujiwara, T. Kobayashi, S. Mizuta, H. Nakashima, *J. Nucl. Sci. Technol.* 39 (8) (2002) 872.
- [5] A. Uehira, S. Ukai, T. Mizuno, T. Asaga, E. Yoshida, *J. Nucl. Sci. Technol.* 37 (9) (2000) 780.
- [6] H. Mimura, T. Ito, E. Yoshida, Y. Tsuchida, S. Kano, I. Nihei, in: LIMET'88, Avignon, 1988, p. 505-1.
- [7] H.U. Borgstedt, C.K. Mathews, *Applied Chemistry of the Alkali Metals*, Plenum, New York, 1987.
- [8] H. Oikawa, *Technology Reports, Tohoku Univ.*, 47 (1) (1982).